far as we know (for intermolecular phenomena, see ref 12, for example).

Molecular Design. Finally, we call the readers' attention to the molecular-design-oriented aspect of this work. In principle, in intramolecular D–A type molecules, relative spatial and symmetry relationships between (among) D and A type groups can be designed and realized much more easily than in intermolecular cases. Moreover, this is also the case for the energetics. For example, by choosing the combination of D and A type groups rather freely it is easy intramolecularly to locate CT bands well separated from local excitation bands so as to make assessments of CT transition moments experimentally with reasonable accuracy. From these standpoints, such D–A type molecules as treated here are quite attractive and fundamentally important for model studies of CT phenomena.

Conclusions

The electronic and orbital structure of DCB and TMDCB has been discussed from various standpoints, the group orbital concept being used as the common basis throughout the discussion. It has been established that the first LU-π-MOs of DCB and TMDCB are almost completely localized on the MN-like moieties from the RP data. The first s–s electronic transition of each compound is an intramolecular CT transition mainly associated with the electron migration from the CHD-like moiety b_2 HO-π-GO to the MN-like moiety a_2 LU-π-GO and provides a typical example of an unusual type of CT transition, a CT transition between the orbitals CT interaction forbidden in the ground state. The mixing coefficients of the component BGOs in the HOMOs of DCB and TMDCB have been evaluated from the PE spectral data and the EA spectral band intensity data, independently from and consistently with each other. The consistency of the mixing coefficients evaluated from the two different standpoints strongly supports the validity of the used models and substantiates the intensity-borrowing model of the first band of each compound from the local allowed π^*–π electronic excitation of the A type group. This conclusion has further been supported by a CM type model consideration for the CT transition moments. This is the first experimental substantiation of intensity borrowing by intramolecular CT bands from local excitations. The CT character of the first band of DCB is enhanced by tetramethylation, and this is mainly ascribed to the destabilization of the basis HO-π-GO of the D type group relative to that of the A type one, therefore, to the enhanced localization of the HOMO onto the D type group by the tetramethylation of DCB. The integration of PE spectroscopy, cyclic voltammetry, EA spectroscopy, and quantum theoretical approaches is very powerful for the multiphased study of molecular electronic structure, in particular, when combined with well molecular-designed model systems as demonstrated in this work.

Experimental and Computational Methods

Materials. 2,3-Dicyanobarrelene (DCB)[13] and its 5,6,7,8-tetramethyl derivative (TMDCB)[8,13] were synthesized according to the methods described in the literature indicated.

Measurements. The gas-phase He I photoelectron spectra of DCB and TMDCB were measured with the instrument described formerly.[14,15] The sample inlet and target chamber systems were heated and kept at 121 °C during the measurements.

The reduction potentials were measured with a Yanaco polarographic analyzer P-1100, Pt wires being used as working and counter electrodes. The solutions contained 0.1 M Et_4NClO_4 supporting electrolyte. The potentials were determined under nitrogen atmosphere at room temperature relative to a saturated calomel electrode (SCE) connected with a salt bridge.

The electronic absorption spectra were measured on a Hitachi 340 recording spectrophotometer.

Computational Details. The CNDO type SCF-MO-CI calculations of DCB and TMDCB were carried out on a FACOM M380 computer at The Institute of Physical and Chemical Research with the method described formerly.[7] All the singly excited configurations between 10 HOMOs and 10 LUMOs were taken into account in the CI calculations. The molecular geometrical structural parameters assumed in the calculations are based on the X-ray diffraction analysis data for TMDCB.[16]

Registry No. DCB, 18341-68-9; TMDCB, 19004-90-1.

(12) (a) Yakushi, K.; Iguchi, M.; Kuroda, H. *Bull. Chem. Soc. Jpn.* **1979**, *52*, 3180. (b) Amano, T.; Kuroda, H.; Akamatsu, H. *Ibid.* **1969**, *42*, 671.

(13) Ciganek, E. *Tetrahedron Lett.* **1967**, 3321.

(14) Kobayashi, T.; Kubota, T.; Ezumi, K. *J. Am. Chem. Soc.* **1983**, *105*, 2172.

(15) Kobayashi, T.; Yokota, K.; Nagakura, S. *J. Electron Spectrosc. Relat. Phenom.* **1973**, *2*, 449.

(16) Nakagawa, A.; Tanaka, J.; Yamochi, H.; Nakasuji, K.; Murata, I., to be submitted for publication.

Isomerization of the Dimethyl Sulfoxide Radical Cation and the Possible Analogies to the Neutral Species

Lars Carlsen* and Helge Egsgaard

Contribution from the Chemistry Department, Risø National Laboratory, DK-4000 Roskilde, Denmark. *Received March 28, 1988*

Abstract: The interconvertibility of the dimethyl sulfoxide (DMSO) radical cation, its proton tautomeric *aci*-DMSO, and methyl methanesulfenate isomers, respectively, has been been investigated by application of collision activation mass spectrometry and metastable ion studies. The isomerization reactions are discussed based on isotopic labeling studies as well as thermodynamical considerations. The interconvertibility of the radical cations of DMSO and *aci*-DMSO as well as the isomerization of the methyl methanesulfenate radical cation into the radical cation of DMSO could be concluded, whereas no unambiguous evidence concerning the possible operation of the DMSO to methyl methanesulfenate isomerization was obtained. Low-pressure gas-phase pyrolysis studies have been applied to elucidate the possible analogies to the corresponding neutral species.

In connection with our continuing interest in isomerization reactions in the gas phase, we recently reported a study on the isomerizations of the nitromethane radical cation in the gas phase[1] as a part of our search for the neutral *aci*-nitromethane. In order to disclose the possible existence of such aci tautomers we are currently studying systems containing "CH_3=X=O" moieties (X = N, P, S), which potentially are able to rearrange into the corresponding aci tautomers "H_2C=X—OH". These studies involve neutral species as well as radical cations.

The present paper describes our studies of the dimethyl sulfoxide system, involving three different structures, which are dimethyl

(1) Egsgaard, H.; Carlsen, L.; Elbel, S. *Ber. Bunsenges. Phys. Chem.* **1986**, *90*, 369-374.

0002-7863/88/1510-6701$01.50/0

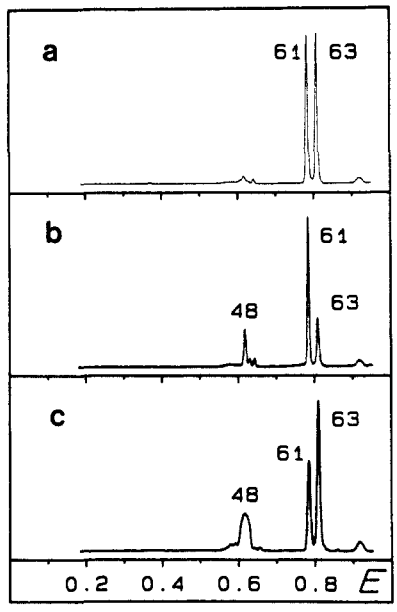

Figure 1. DADI spectra of the electron-impact-induced molecular ions of (a) DMSO (**4**), (b) *aci*-DMSO (**5**), and (c) methyl methanesulfenate (**6**).

sulfoxide (**1**), *aci*-dimethyl sulfoxide (**2**), and methyl methanesulfenate (**3**) as well as the corresponding radical cations **4**–**6**.

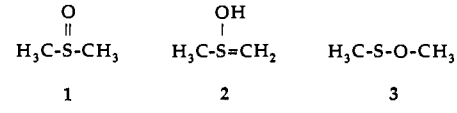

1 2 3

Primarily reactions proceeding on the potential surface belonging to the ionized species have been studied. The possible analogies to reactions taking place on the ground-state potential surface are discussed in the final part of the paper.

Reference Structures

The necessary reference structures for the studies of the isomerization reactions of the DMSO radical cation were easily obtained. The DMSO radical cation (**4**) as well as the methyl methanesulfenate radical cation (**6**) were obtained by direct ionization of the corresponding neutral species. The neutral methyl methanesulfenate (**3**) was synthesized in a reaction between (phthalimidothio)methane (**7**) and methoxide ions. The radical cation of the *aci*-DMSO structure (**5**) was obtained as an electron-impact-induced fragment ion of the radical cation of methyl carboxymethyl sulfoxide (**8**), the neutral species, i.e., methyl carboxymethyl sulfoxide (**9**) being synthesized by simple peracid oxidation of the corresponding sulfide (**10**).

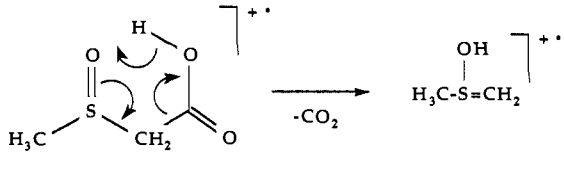

8 5

The three reference structures **4**, **5**, and **6** have been characterized based on their unimolecular fragmentation patterns (DADI), as well as on the collisional induced fragmentations (CA). The resulting spectra are depicted in Figures 1 and 2, respectively. It is unambiguously demonstrated (Figures 1 and 2) that all three isomeric structures (m/z 78) are characterized by the appearance of two peaks corresponding to losses of OH$^\bullet$ (m/z 61) and $CH_3^\bullet$ (m/z 63) from the respective molecular ions as previously stated in the case of DMSO.[2] However, both the DADI as well as the

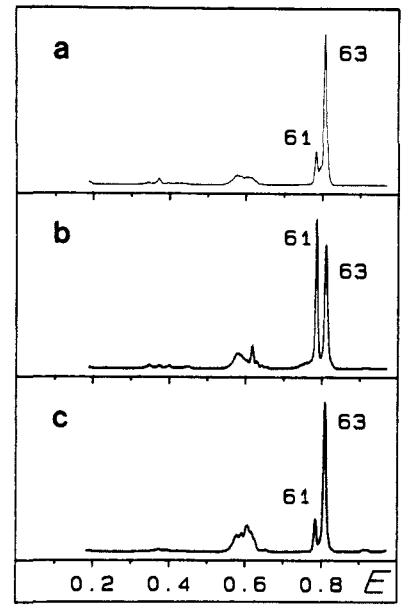

Figure 2. CA mass spectra of the electron-impact-induced molecular ions of (a) DMSO (**4**), (b) *aci*-DMSO (**5**), and (c) methyl methanesulfenate (**6**).

Table I. MNDO Calculated Bond Orders and Charge Densities

	bond orders[a]				
	CH_3–O	CH_3–S	CH_2–S	S–O	O–H
DMSO (**1**)		0.87		1.18	
DMSO$^{\bullet+}$ (**4**)		0.77		1.25	
aci-DMSO (**2**)		0.86	1.33	0.64	0.95
aci-DMSO$^{\bullet+}$ (**5**)		0.85	1.02	0.95	0.92
MeSOMe (**3**)	0.87	0.97		0.96	
MeSOMe$^{\bullet+}$ (**6**)	0.90	0.95		1.10	
	charge densities[b]				
	C(H3)(O)	C(H3)(S)	C(H2)(S)	S(C)(O)	O(S)(H)
DMSO (**1**)		−0.12		+0.68	−0.64
DMSO$^{\bullet+}$ (**4**)		+0.05		+0.51	−0.16
aci-DMSO (**2**)		−0.13	−0.60	+0.78	−0.49
aci-DMSO$^{\bullet+}$ (**5**)		+0.01	−0.08	+0.59	−0.31
MeSOMe (**3**)	+0.19	−0.01		+0.09	−0.33
MeSOMe$^{\bullet+}$ (**6**)	+0.17	−0.02		+0.58	−0.24

[a] C–H bond orders not given in the table. [b] Charges on the hydrogen atoms are not given in the table.

CA spectra exhibit distinct differences in the mutual m/z 61:63 ratio as well as in the composite peak around m/z 48. Hence, the three structures can unequivocally be identified by these techniques.

Obviously the CA spectra typically exhibit increased m/z 63:61 ratios over the corresponding DADI spectra. Since the collision activation, the more probable collision energy being around 1 eV,[3] favors more energy-demanding fragmentations, compared to the pure unimolecular fragmentations (DADI), we conclude that the loss of methyl radicals apparently is somewhat more energy demanding than that of the hydroxy radical loss. However, it should be remembered that in contrast to the loss of OH$^\bullet$, which most probably proceeds via a common structure in all three cases, the methyl radical loss may well take place through different channels for the different structures. This shall be discussed in detail below.

We also carried out semiempirical MNDO calculations on the involved structures, neutral as well as ionized. The calculated bond orders and charge densities for the six structures **1**–**6** are given in Table I. The figures given in the table display a series of interesting features. In the case of DMSO, ionization causes a slight weakening of the C–S bonds, indicated by the somewhat lower C–S bond order. Simultaneously, a slight increase of the

(2) Griffiths, I. W.; Howe, I.; March, R. E.; Beynon, J. H. *Int. J. Mass Spectrom. Ion Processes* **1983**, *54*, 323–332.

(3) Carlsen, L.; Egsgaard, H. *Thermochim. Acta* **1980**, *38*, 47–58.

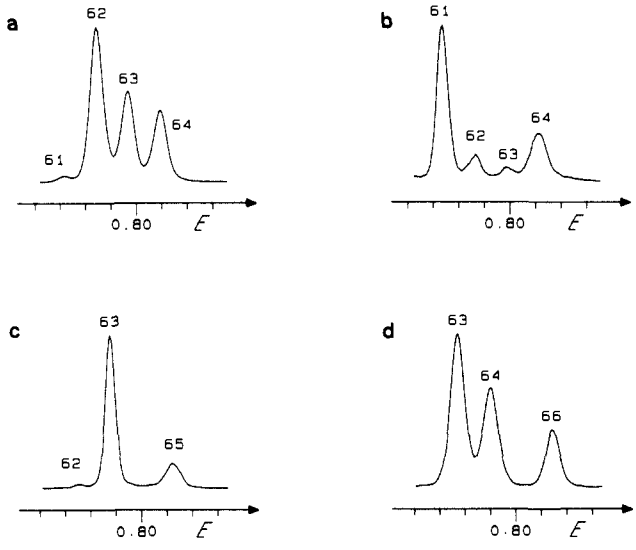

Figure 3. Partial CA mass spectra of the electron-impact-induced molecular ions of the deuterium-labeled species **4'**, **5'**, **5''**, and **6'**.

S–O bond order can be noted. The figures given for the charge densities disclose, not unexpected, that the sulfur atom bears the major part of the positive charge. This is true for both the neutral as well as the ionized DMSO. The significant change in charge distribution upon ionization occurs at the oxygen atom.

The calculated bond orders for the *aci*-DMSO structures disclose some rather surprising features. It is noted that the neutral *aci*-DMSO exhibits a semipolar H_2C–S bond (bond order = 1.33), which is further verified by the calculated charge densities which were found to be −0.60 and +0.78 for the carbon and sulfur atom, respectively. Comparison between the bond orders of the sulfur atom and the oxygen and the methyl group, respectively, strongly suggests that the sulfur atom effectively still is trivalent. Hence, we conclude that the *aci*-DMSO exhibits an ylide-like structure. The *aci*-DMSO radical cation likewise appears to contain a trivalent sulfur atom as the bond orders for all three bonds to this atom approach unity. As was the case of the DMSO radical cation, the positive charge is concentrated on the sulfur atom. Not surprisingly both the neutral and the ionized *aci*-DMSO structures display a pronounced charge separation over the O–H bond. In the third type of structures, i.e., the sulfenates, it shall only be mentioned that again the sulfur atom bears the larger part of the positive charge in the radical cation.

Interconversion

As demonstrated by the DADI as well as by the CA spectra (vide supra), the two dominant fragmentation processes for the three structures **4**–**6** were the losses of $CH_3^\bullet$ and $OH^\bullet$, respectively. It appears obvious that the $OH^\bullet$ loss of necessity must proceed via a structure exhibiting an OH moiety. The apparent common OH-bearing structure can undisputably be argued as the *aci*-DMSO radical cation (**5**). Hence, we conclude the existence of **4** → **5** as well as **6** → **5** isomerizations. In addition we strongly emphasize the obvious intermediacy of the DMSO radical cation **4** in the **6** → **5** isomerization. Studies on the corresponding deuterium-labeled species (vide infra) furthermore demonstrated the operation of an **5** → **4** isomerization. On the other hand, we have not been able to achieve any conclusive evidence as to the operation of a **4** → **6** isomerization. However, thermodynamical considerations (vide infra) certainly do not rule out the existence of such a reaction.

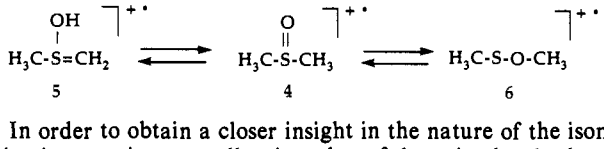

In order to obtain a closer insight in the nature of the isomerization reactions as well as into that of the unimolecular losses

Scheme I

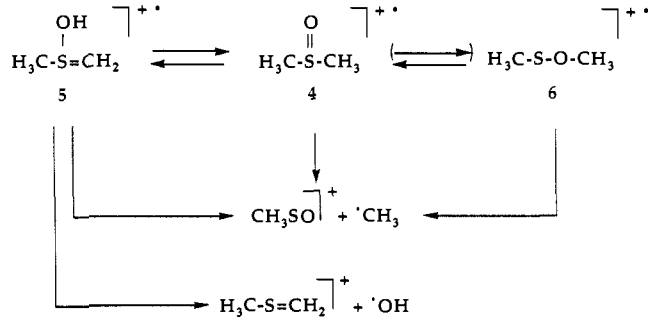

of $CH_3^\bullet$ and $OH^\bullet$, we carried out a series of deuterium-labeling experiments. These studies included the radical cations of monodeuterated DMSO (**4'**), OD-*aci*-DMSO (**5'**), the D_2-*aci*-DMSO (**5''**), and the trideuteromethyl methane sulfenate (**6'**)).

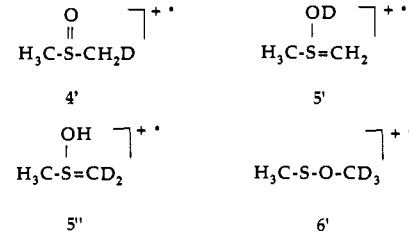

The partial DADI spectra of the structures **4'**, **5'**, **5''**, and **6'** are depicted in Figure 3.

The isomerization of DMSO into *aci*-DMSO can be recognized (Figure 3a), as both a loss of $OD^\bullet$ and $OH^\bullet$, giving rise to the peaks of m/z 61 and 62, can be seen. Furthermore, the isotopic effect can directly be obtained as the m/z 62:61 ratio. Based on the spectrum given in Figure 3a, a moderate hydrogen–deuterium isotope effect was disclosed, K_H/K_D being estimated to 4.9. It should be noted that an m/z 62:61 ratio equal to 5 would have indicated a zero isotope effect, i.e., $K_H/K_D = 1$. It is interesting to note this rather small isotope effect compared to the nitromethane/*aci*-nitromethane system, where K_H/K_D was estimated to be higher than 50,[1] strongly indicating the operation of quantum-mechanical tunneling in the latter case. This difference most probably reflects the much higher flexibility of the bond angles around sulfur than those around nitrogen. It is in this context important to note that all three bonds to sulfur in the *aci*-DMSO apparently are single bonds (vide supra). Concerning the loss of the methyl radical, the expected equality of the CH_3 and the CH_2D groups is reflected by the appearance of the two peaks m/z 64 and 63 of equal intensity.

In contrast to this the spectrum given in Figure 3b clearly demonstrates that the methyl radical loss in the case of the *aci*-DMSO radical cation is a direct $CH_3^\bullet$ loss, giving rise to m/z 64, thus not involving a primary isomerization to the DMSO radical cation. If this had been the case, equal intensity peaks of m/z 64 and 63, corresponding to $CH_3^\bullet$ and $CH_2D^\bullet$ losses, would have appeared. On the other hand, the minor peaks of m/z 63 (loss of $CH_2D^\bullet$) and m/z 62 (loss of $OH^\bullet$) reflect the existence of a **5'** ⇄ **4'** isomerization. This is further confirmed through scrutinizing the DADI spectrum of **5''** (Figure 3c), which virtually exhibits peaks at m/z 65 and 63 only, corresponding to loss of $CH_3^\bullet$ and $OH^\bullet$, respectively.

The reaction of the methyl methane sulfenate radical cation can be deducted from the spectrum depicted in Figure 3d. This spectrum is dominated by three major peaks of m/z 63, 64, and 66, respectively. The two peaks of m/z 63 and 66 can be rationalized as losses of $CD_3^\bullet$ and $CH_3^\bullet$, respectively, whereas m/z 64 apparently is a result of loss of $OH^\bullet$. A priori a contribution to m/z 63 due to an $OD^\bullet$ loss should be considered. However, owing to the isotope effects outlined above, we concluded that this contribution can be considered as vanishingly small. Based on the above discussions a reaction scheme elucidating the rearrangements/investigations and fragmentations of the DMSO

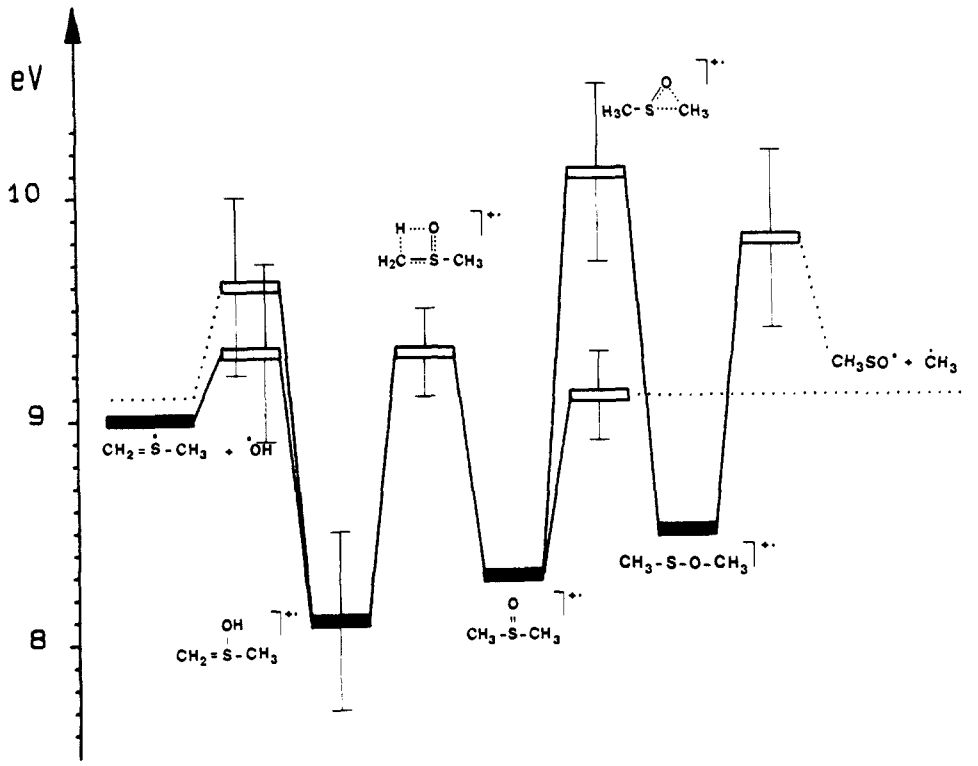

Figure 4. Semiquantitative energy diagram of rearrangements and fragmentations of the DMSO radical cation system. Estimated uncertainties are visualized by vertical bars.

Table II. Kinetic Energy Release (KER) (meV) for $CH_3^{\bullet}$ and $HO^{\bullet}$ Losses (Given as $T_{50\%}$ Values)

	$OH^{\bullet}$ los	$CH_3^{\bullet}$ loss
$DMSO^{\bullet+}$	22[a]	19[a]
aci-$DMSO^{\bullet+}$	8	29
$MeSOMe^{\bullet+}$	36	30

[a] Identical with data available in the literature.[2]

radical cation system can be constructed (See Scheme I).

Thermochemical Aspects

In order to obtain a quantitatively somewhat more detailed outline of the qualitative reaction scheme given above, we carried out a semiquantitative analysis of the potential energy surface, the results being supported by kinetic energy release (KER) data. The reason for considering the thermochemical analysis as being semiquantitative has to be sought for in the following facts. (a) Only part of the necessary ground-state heat-of-formation (ΔH_f) values is available in the literature. Thus ΔH_f values for **3** and **9** had to be estimated by other methods (cf. Experimental Section). (b) ΔH_f(**5**) could be determined only with considerable uncertainties, owing to significant reverse activation energy for the reaction **8** → **5**. (c) Only low ion currents of **5** and **6** could be obtained because of the pronounced lability of the species **3** and **9**, respectively. The energies of the transition states are based on the AE's of the metastable ions and the AE's of the corresponding ground states and correction for the KER. In Figure 4 the potential energy surface, as a result of the semiquantitative analysis outlined above, is visualized. **Note Added in Proof**: For improved thermochemical data of Zha et al., see: Zha, Q.; Nishimura, T.; Geisels, G. G. *Int. J. Mass Spectrom. Ion Processes* **1988**, *83*, 1–12.

The thermochemical considerations leading to the potential energy surface appear to be supported by studies on kinetic energy release (KER) during the loss of hydroxy radicals, whereas the data obtained for the methyl radical losses should be taken with caution as these losses, as demonstrated above, originate from different pathways. Thus, in the latter case only KER data of the $CH_3^{\bullet}$ loss from **4** and **6** can be compared. In Table II KER data for $CH_3^{\bullet}$ and $OH^{\bullet}$ losses from **4**, **5**, and **6** are given as $T_{50\%}$ values.

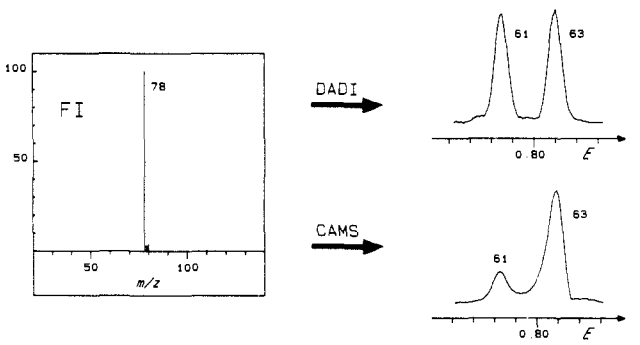

Figure 5. Field ionization mass spectrum of the gaseous pyrolysis product obtained following pyrolysis at 883 K of methyl carboxymethyl sulfoxide and partial DADI and CA spectra of the electron-impact-induced molecular ion m/z 78.

Neutral *aci*-DMSO?

In contrast to the neutral species **1** and **3**, *aci*-DMSO is apparently not a subject for traditional organic synthesis. Hence, gas-phase pyrolysis may a priori well constitute an advantageous alternative route to **2**, the above-described studies enabling us, by means of mass spectrometric techniques, to disclose a possible formation of the latter. The pyrolysis studies were carried out applying the Curie-point pyrolysis–field ionization mass spectrometry technique described in detail in previous papers.[3,4]

Taking the above-described studies into account, two obvious strategies for pyrolytic formation of *aci*-DMSO were developed. These are (1) pyrolysis of DMSO expectably causing an intramolecular isomerization to the aci tautomer, and (2) pyrolysis of methyl carboxymethyl sulfoxide (**9**), hoping for a thermally induced CO_2 extrusion analoguously to the observed electron-impact-induced fragmentation.

We have previously studied the gas-phase pyrolytic reactions of DMSO.[5,6] However, no indication of a **1** → **2** isomerization

(4) Egsgaard, H.; Larsen, E.; Carlsen, L. *J. Anal. Appl. Pyrolysis* **1982**, *4*, 33–46.
(5) Egsgaard, H.; Carlsen, L. *J. Anal. Appl. Pyrolysis* **1983**, *5*, 1–7.
(6) Carlsen, L.; Egsgaard, H.; Harpp, D. N. *J. Chem. Soc., Perkin Trans. 2* **1981**, 1166–1170.

was observed, whereas indirect evidence for a **1** → **3** isomerization was noted.

Pyrolysis of **9** at 883 K gave rise to formation of a species with a molecular weight corresponding to DMSO/*aci*-DMSO as visualized by the appearance of an *m/z* 78 peak in the FI mass spectrum obtained following pyrolysis (Figure 5). However, the DADI as well as the CA spectrum of the *m/z* 78 (cf. Figure 5 with Figures 1 and 2) unambiguously demonstrated that the *m/z* 78 should be assigned to DMSO.

It appears as a reasonable suggestion that the primary product upon pyrolysis of **9** indeed is the *aci*-DMSO (**3**); the isomerization

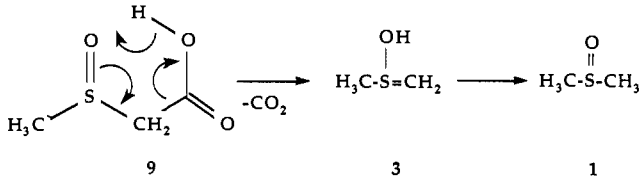

9 3 1

to DMSO (**1**), however, is rapid compared to the transfer time from the pyrolysis reaction to the ion source of the mass spectrometer.[7] Since the possible **3** → **1** isomerization most probably is induced by molecular-surface collisions in the pyrolyzer–ion source interface, it appears that molecular-beam MS/MS is required to prove the intermediary existence of neutral *aci*-DMSO in the above-described experiment. An obvious alternative is neutralization of the radical cation **5** to **3**. Neutralization–reionization/mass spectrometry (NR/MS)[8,9] has been proven as the optimal choice in the case of *aci*-nitromethane.[10]

Experimental Section

MS Experiments. The mass spectrometric investigations were carried out using a Varian MAT CH 5D double-focusing spectrometer equipped with a combined EI/FI/FD ion source. Field ionization spectra were obtained using a 10-μm tungsten wire, activated in benzonitrile vapor, as emitter.

Unimolecular fragmentation processes occurring in the second field-free region were detected by the DADI (direct analysis of daughter ions) technique. Collision activation was carried out by introducing He as target gas.[3,4] The CA spectra are uncorrected for unimolecular processes. Kinetic energy release was determined from the width of the peak at half-height and corrected for the energy spread of the main beam.

Flash Vacuum Pyrolysis. Low-pressure pyrolysis was carried out using the gas-phase Curie-point pyrolysis technique as described in detail previously.[3,4] Gold-plated filaments were applied to suppress possible surface-promoted reactions.[5]

Data Processing. All data were acquired via a HP3497A data acquisition/control unit and a HP3956A digital voltmeter and processed on a HP9836 computer. Signal averaging, combined with digital filtering, was applied in order to study weak signals satisfactorily.

Thermochemistry. Appearance energies (AE) were derived from plots of ion currents vs. nominal electron energy. The energy scale was calibrated by the measurement of a series of ionic species with well-defined appearance/ionization energies within the actual energy domain, the onset being determined on the basis of "vanishing current". Thus, the heat of formation of **5** was determined from the appearance energy of **5** (E_A = 9.8 eV) arising from **8**: $\Delta H_f(\mathbf{5}) = E_A(\mathbf{5}) + \Delta H_f(\mathbf{8}) - \Delta H_f(CO_2) - \epsilon$. $\Delta H_f(\mathbf{8})$ = -5.4 eV was estimated based on the group additivity method by Benson,[11] $\Delta H_f(CO_2)$ = -4.1 eV,[12] and the reverse activation energy ϵ = 0.35 eV (KER data) leading to $\Delta H_f(\mathbf{5}) \approx 8.1$ eV. $\Delta H_f(\mathbf{4})$ = 8.3 eV was determined from E_i = 9.8 eV and $\Delta H_f(\mathbf{2})$ = -1.5 eV ("Benson-derived" value). $\Delta H_f(\mathbf{6})$ was estimated to be ≈8.5 eV, based on the "addition-principle"[13] using MeOH/MeSH and MeOOMe/MeSSMe as basis set. The critical energies for dissociations were obtained directly from the appearance energies of the appropriate metastable ions: **5** → CH_3—S=CH_2^+ + OH•, 1.2 eV; **5** → CH_3SO^+ + •CH_3, 1.5 eV; **4** → CH_3—S=CH_2^+ + OH•, 1.0 eV; **4** → CH_3SO^+ + •CH_3, 0.8 eV; **6** → CH_3—S=CH_2^+ + OH•, 1.6 eV; **6** → CH_3SO^+ + •CH_3, 1.3 eV. The heat of formation $\Delta H_f(CH_3$—S=CH_2^+ + OH•) was obtained from $\Delta H_f(CH_3$—S=CH_2^+) = 8.6 eV[14] and ΔH_f(•OH) = 0.4 eV.[12]

Chemicals. Methyl Methanesulfenate (3). To a suspension of 5 g of (phthalimidodithio)methane (**7**) in 25 mL of methanol, 0.6 g of elemental sodium in 10 mL of methanol was added (0 °C/N_2). Samples from the reaction mixture were introduced directly via the gas-inlet system of the mass spectrometer kept at ambient temperature. Field ionization mass spectrometry disclosed the presence of **3** as the only gaseous product.

Trideuteriomethyl methanesulfenate was prepared analoguously applying CD_3OD.

Methyl carboxymethyl sulfoxide (9) was obtained by peracid oxidation (0.1 mL of 30% H_2O_2/0.5 mL of acetic anhydride) of the corresponding sulfide (**10**) (commercially available) at 0 °C (15 min). Samples were analyzed using the direct inlet system of the mass spectrometer kept at ~20 °C.

OD-labeled methyl carboxymethyl sulfoxide was prepared by H–D exchange (D_2O) of **9**, whereas the CD_2 analogue was prepared as described for **9**, the corresponding sulfide CH_3SCD_2COOH being obtained by H–D exchange of **10** (D_2O/NaOD, 100 °C, 1 h).

The methyl carboxymethyl sulfoxides should be handled at temperatures as low as possible because of a pronounced tendency to self-condensation, a reaction which also made attempts to isolate the pure compounds difficult.

(7) Egsgaard, H.; Carlsen, L. *J. Anal. Appl. Pyrolysis* **1984**, *7*, 1–13.
(8) Wesdemiotis, C.; McLafferty, F. *Chem. Rev.* **1987**, *87*, 485–500.
(9) Terlouw, J. K.; Schwarz, H. *Angew. Chem.* **1987**, *99*, 829–839.
(10) Egsgaard, H.; Carlsen, L.; Florencio, H.; Drewello, T.; Schwarz, H., submitted for publication.
(11) Benson, S. W. *Thermochemical Kinetics. Methods for the Estimation of Thermochemical Data and Rate Parameters*, 2nd ed.; Wiley: New York, 1976.
(12) Rosenstock, H. M.; Draxl, K.; Steiner, B. W.; Herron, J. T. *J. Phys. Chem. Ref. Data*, **1977**, *6*, Suppl. 1.
(13) Holmes, J. L.; Lossing, F. P. *Can. J. Chem.* **1982**, *60*, 2365–2371.
(14) Broer, W. J.; Weringa, W. D.; Nieuwpoort, W. C. *Org. Mass Spectrom.* **1979**, *14*, 543–549.